online data

AMP-activated protein kinase-independent inhibition of hepatic mitochondrial oxidative phosphorylation by AICA riboside

Bruno GUIGAS*[1], Nellie TALEUX*†, Marc FORETZ‡§, Dominique DETAILLE†, Fabrizio ANDREELLI‡§, Benoit VIOLLET‡§ and Louis HUE*

*Université catholique de Louvain and Institute of Cellular Pathology, Hormone and Metabolic Research Unit, Brussels, Belgium, †Bioénergétique Fondamentale et Appliquée INSERM-EMI0221, Université J. Fourier, Grenoble, France, ‡Institut Cochin, Université Paris Descartes, CNRS (UMR 8104), Paris, France, and §Inserm, U567, Paris, France

AICA riboside (5-aminoimidazole-4-carboxamide-1-β-D-ribofuranoside) has been extensively used in cells to activate the AMPK (AMP-activated protein kinase), a metabolic sensor involved in cell energy homoeostasis. In the present study, we investigated the effects of AICA riboside on mitochondrial oxidative; phosphorylation. AICA riboside was found to dose-dependently inhibit the oligomycin-sensitive JO_2 (oxygen consumption rate) of isolated rat hepatocytes. A decrease in P_i (inorganic phosphate), ATP, AMP and total adenine nucleotide contents was also observed with AICA riboside concentrations > 0.1 mM. Interestingly, in hepatocytes from mice lacking both $\alpha 1$ and $\alpha 2$ AMPK catalytic subunits, basal JO_2 and expression of several mitochondrial proteins were significantly reduced compared with wild-type mice, suggesting that mitochondrial biogenesis was perturbed. However, inhibition of JO_2 by AICA riboside was still present in the mutant mice and thus was clearly not mediated by AMPK. In permeabilized hepatocytes, this inhibition was no longer evident, suggesting that it could be due to intracellular accumulation of Z nucleotides and/or loss of adenine nucleotides and P_i. ZMP did indeed inhibit respiration in isolated rat mitochondria through a direct effect on the respiratory-chain complex I. In addition, inhibition of JO_2 by AICA riboside was also potentiated in cells incubated with fructose to deplete adenine nucleotides and P_i. We conclude that AICA riboside inhibits cellular respiration by an AMPK-independent mechanism that likely results from the combined intracellular P_i depletion and ZMP accumulation. Our data also demonstrate that the cellular effects of AICA riboside are not necessarily caused by AMPK activation and that their interpretation should be taken with caution.

Key words: AICA riboside, AMP-activated protein kinase (AMPK), hepatocyte, mitochondrial biogenesis, mitochondrial oxidative phosphorylation, ZMP.

INTRODUCTION

AICA riboside (5-aminoimidazole-4-carboxamide-1-β-D-ribofuranoside) is the nucleoside corresponding to AICA ribotide (AICAR or ZMP), the antepenultimate metabolic intermediate of the *de novo* purine synthesis pathway. Although strictly speaking, AICAR refers to the nucleotide (AICA ribotide or ZMP, with Z referring to imidazole), it is however often used to designate the corresponding nucleoside (AICA riboside). To avoid any confusion, in the present study we use AICA riboside and ZMP. AICA riboside shares some structural similarities with adenosine and enters certain cell types to be phosphorylated into ZMP by adenosine kinase [1,2]. ZMP is an analogue of AMP and mimics several of the cellular effects of this adenine nucleotide. In recent years, AICA riboside has been extensively used in cells [3,4] or even *in vivo* [5–9] to activate the AMPK (AMP-activated protein kinase) and assess its function in a large number of pathways.

AMPK is a heterotrimeric protein kinase consisting of a catalytic (α) and two regulatory subunits (β and γ) (see [10,11] for recent reviews). Considered as a metabolic 'fuel gauge', AMPK becomes activated by changes in intracellular adenine nucleotide concentrations, namely a fall in ATP with the resulting increase in AMP concentration that occurs in cells submitted to environmental and nutritional stresses. In the presence of AMP (or ZMP), AMPK can be phosphorylated on Thr^{172} which is located in the activation loop of its catalytic subunit. This activating phosphorylation can be catalysed by either LKB1 or the Ca^{2+}/calmodulin-dependent protein kinase kinase β, two protein kinases located upstream of AMPK [10]. Once activated, AMPK inactivates energy-consuming biosynthetic pathways and activates ATP-producing catabolic pathways, thereby maintaining cellular ATP levels. The importance of the role of AMPK in the control of energy homoeostasis is further underlined by its indirect stimulatory effect on mitochondrial biogenesis [12], at least in skeletal muscle [13,14].

We recently reported that AICA riboside inhibited the glucose-induced translocation of glucokinase from the nucleus to the cytosol in hepatocytes by a mechanism that could be related to a decrease in intracellular ATP concentrations [15]. Therefore one could wonder whether AICA riboside could affect mitochondrial ATP production, and whether this effect is mediated by AMPK. The aim of the present study was to test this hypothesis by studying the effects of AICA riboside on the mitochondrial OXPHOS (oxidative phosphorylation) pathway in hepatocytes from both rat and wild-type or newly engineered liver-specific $AMPK\alpha_1\alpha_{2LS}^{-/-}$ mice.

MATERIALS AND METHODS

All procedures were performed in accordance with the principles and guidelines established by the European Convention for the Protection of Laboratory Animals.

Abbreviations used: ACC, acetyl-CoA carboxylase; AICA riboside, 5-aminoimidazole-4-carboxamide-1-β-D-ribofuranoside; AMPK, AMP-activated protein kinase; COX, cytochrome oxidase; DNP, 2,4-dinitrophenol; Fru-1-P, fructose 1-phosphate; Gly-3-P, glycerol 3-phosphate; JO_2, oxygen consumption rate; OXPHOS, oxidative phosphorylation; PGC-1α, peroxisome activated receptor γ coactivator-1α; P_i, inorganic phosphate; RT, reverse transcriptase; TMPD, N, N, N′, N′-tetramethyl-1, 4-phenylenediamine; ZMP, AICA ribotide.

[1] To whom correspondence should be addressed (email: b.guigas@lumc.nl).

Generation of AMPK$\alpha_1\alpha_{2LS}^{-/-}$ knockout mice

To obtain a deletion of both catalytic subunits in the liver (AMPK$\alpha_1\alpha_{2LS}^{-/-}$), we first generated a liver-specific AMPKα_2-null mouse (AMPK$\alpha_2^{-/-}$) by crossing floxed AMPKα_2 mice [16] and an AlfpCre transgenic line expressing the Cre recombinase under the control of the albumin and α-fetoprotein regulatory elements [17]. We then produced a liver-specific AMPK$\alpha_1\alpha_{2LS}^{-/-}$ mouse on an AMPK$\alpha_1^{-/-}$ background by crossing liver-specific AMPK$\alpha_2^{-/-}$ mice with AMPK$\alpha_1^{-/-}$ mice [18]. Mice were genotyped using PCR on DNA extracted from a tail biopsy using specific primers for the Cre transgene and for the floxed AMPKα_2, the deleted AMPKα_1 and the wild-type AMPKα_1 gene.

Isolation of hepatocytes

Liver cells were prepared using the collagenase method [19] from male Wistar rats (200–300 g) or from male mice (25–30 g) after anaesthesia with sodium pentobarbital (6 mg per 100 g of body mass) or ketamin/xylazin (8 mg and 1 mg respectively per 100 g of body mass).

Isolation of rat mitochondria

Liver mitochondria from male Wistar rats (200–300 g) were prepared in sucrose medium [250 mM sucrose, 1 mM EGTA and 20 mM Tris/HCl (pH 7.2)] according to the standard method described by Klingenberg and Slenczka [20]. Mitochondrial proteins were estimated by the Biuret method using BSA as a standard.

Determination of mitochondrial oxygen consumption rate in intact and permeabilized hepatocytes, and isolated mitochondria

Rat or mouse hepatocytes (7–8 mg of dry cells $\cdot$ ml^{-1}) were incubated in a shaking water bath at 37 °C in closed vials containing 2 ml of Krebs–Ringer bicarbonate calcium buffer [120 mM NaCl, 4.8 mM KCl, 1.2 mM KH_2PO_4, 1.2 mM $MgSO_4$, 24 mM $NaHCO_3$ and 1.3 mM $CaCl_2$ (pH 7.4)] supplemented with the indicated concentrations of substrates and AICA riboside, and in equilibrium with a gas phase containing O_2/CO_2 (19:1). At the indicated times, the cell suspension was saturated again with O_2/CO_2 for 1 min and immediately transferred into a stirred oxygraph vessel equipped with a Clark oxygen electrode. The JO_2 (oxygen consumption rate) was measured at 37 °C before and after successive addition of 0.5 μM oligomycin, 150 μM DNP (2,4-dinitrophenol), 0.15 μg/ml antimycin and 1 mM TMPD (N,N,N′,N′-tetramethyl-1,4-phenylenediamine) plus 5 mM ascorbate.

To permeabilize hepatocytes, intact cells from mice (7–8 mg of dry cells $\cdot$ ml^{-1}) were first incubated for 30 min as described above, then harvested by centrifugation (2000 ***g*** for 10 s) and resuspended in KCl medium [125 mM KCl, 20 mM Tris/HCl, 1 mM EGTA and 5 mM P_i/Tris (pH 7.2)] containing 200 μg/ml digitonin. After 3 min at 37 °C, the permeabilized hepatocytes were transferred to the oxygraph vessel. As indicated, 5 mM glutamate/Tris plus 2.5 mM malate/Tris or 5 mM succinate/Tris plus 0.5 mM malate/Tris plus 1.25 μM rotenone were added. JO_2 was measured before and after the successive additions of 1 mM ADP/Tris, 0.5 μg/ml oligomycin, 50 μM DNP, 0.15 μg/ml antimycin and 1 mM TMPD plus 5 mM ascorbate, to determine the phosphorylating (state 3), the non-phosphorylating (state 4) and the uncoupled respiratory rate, and the maximal activity of cytochrome oxidase respectively. In all experiments, the antimycin-sensitive JO_2, which corresponds to mitochondrial respiration, was calculated by subtracting the antimycin-insensitive JO_2 from the total JO_2.

For mitochondrial experiments, isolated rat mitochondria (1 mg of protein $\cdot$ ml^{-1}) were incubated at 37 °C in the oxygraph vessel containing 2 ml of the KCl medium (described above) in the presence of 1 mM AICA riboside or the indicated concentrations of ZMP and ZTP. After equilibration for 30 s, the mitochondrial respiratory rate was monitored in the presence of glutamate/malate or succinate/malate/rotenone, as described above for permeabilized hepatocytes.

Determination of complex I and citrate synthase activities

The specific activity of the respiratory-chain complex I was assessed in disrupted mitochondria following hypoosmotic shock by the rotenone-sensitive oxidation rate of NADH in the presence of decylubiquinone as an electron acceptor [21]. Citrate synthase activity was measured on liver homogenate, as described previously [22]. The activities are expressed as nmol $\cdot$ min^{-1} $\cdot$ mg of protein^{-1} (complex I) or μmol $\cdot$ min^{-1} $\cdot$ g of protein^{-1} (citrate synthase), the protein contents being determined using the Pierce BCA kit.

Determination of nucleotides and P_i concentrations, and of gluconeogenesis and ketogenesis

After 30 min of incubation, samples of the cell suspension were quenched in ice-cold 25 mM $HClO_4$ [5 % (w/v)]/25 mM EDTA and centrifuged (13 000 ***g*** for 2 min). The supernatants were neutralized and adenine nucleotides, ZMP and AICA riboside concentrations were measured by HPLC [23]. To measure intracellular P_i, a 0.7 ml sample of the cell suspension was centrifuged (13 000 ***g*** for 1 min) through a silicon oil layer into 0.25 ml of $HClO_4$ [10 % (w/v)]/25 mM EDTA. P_i was measured colorimetrically [24]. For gluconeogenesis and ketogenesis measurements, samples of the cell suspension were quenched in ice-cold $HClO_4$ [5 % (w/v)], centrifuged (13 000 ***g*** for 2 min) and the supernatants were neutralized. Glucose, acetoacetate and β-hydroxybutyrate concentrations were measured using enzymatic methods coupled with spectrophotometric determinations of NADH, as described previously [23].

AMPK assay

Total AMPK activity from hepatocyte extracts was assayed after precipitation with 10 % (w/v) poly(ethylene glycol) 6000 [15].

Western blot analysis

Expression of cytochrome *c* and COX (cytochrome oxidase) subunit IV and the phosphorylation state of ACC (acetyl-CoA carboxylase) were monitored by SDS/PAGE immunoblots with anti-cytochrome *c* (clone 7H8.2C12; BD Biosciences), anti-cytochrome oxidase, subunit IV (Cell Signaling) and anti-phosphoSer79 ACC (Upstate) antibodies respectively. Expression of α-actin (Santa Cruz) was used as a loading control. Quantification was performed by densitometry using Image J 1.32 (National Institutes of Health).

RNA purification and quantitative RT (reverse transcription)-coupled real-time PCR

Total RNA was isolated with RNA+ (Qbio-gene), and single-strand cDNA was synthesized from 5 μg of total RNA with random hexamer primers and Superscript II (Invitrogen). Real-time RT-PCRs were performed using a LightCycler reaction kit (Eurogentec) in a final volume of 20 μl containing 250 ng of reverse-transcribed total RNA, 500 nmol $\cdot$ l^{-1} of primers, 10 μl of 2× PCR mix and 0.5 μl of SYBR® Green. The reactions were performed in a LightCycler instrument (Roche) using 40 cycles. The relative amounts of the mRNAs studied were determined

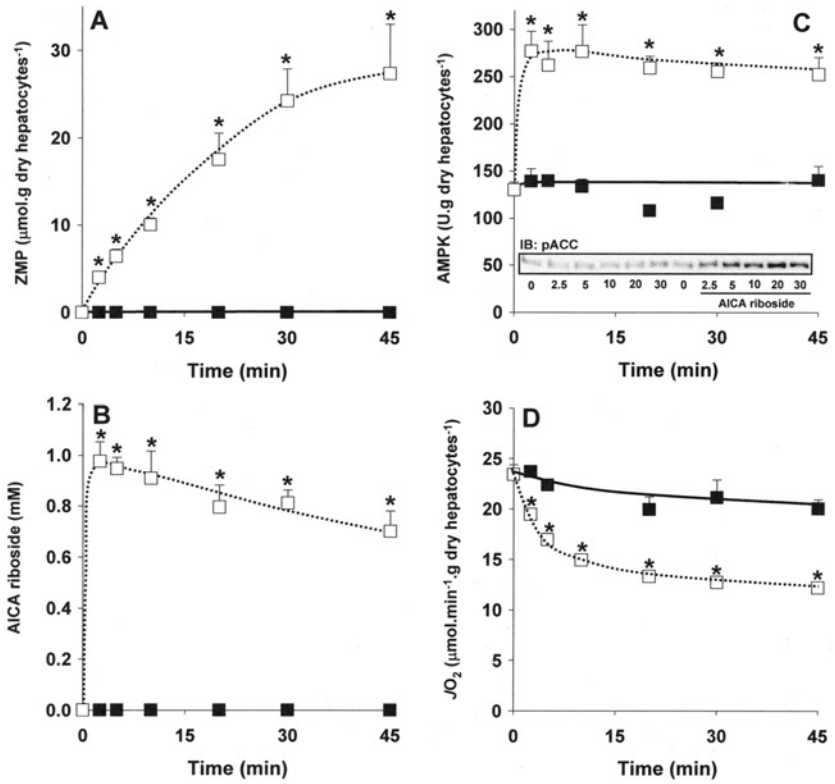

Figure 1 Time-course of the effects of AICA riboside on intracellular ZMP concentration, AMPK activity and JO_2 in rat hepatocytes

Hepatocytes isolated from 24 h-starved rats were incubated at 37 °C in a Krebs/bicarbonate medium supplemented with 20 mM lactate, 2 mM pyruvate and 4 mM octanoate. After 15 min of pre-incubation (zero time), AICA riboside (1 mM final concentration, □) or its vehicle (■) were added and cell samples were removed at the indicated time for determination of intracellular ZMP content (**A**), AICA riboside concentration in the medium (**B**), AMPK activity (**C**) and phosphorylation state of ACC on Ser^{79} (**C**, inset). The JO_2 was measured in separate experiments before and after the addition of 0.15 μg/ml antimycin. The antimycin-sensitive JO_2 was calculated by subtracting the antimycin-insensitive JO_2. The results are expressed as means ± S.E.M. ($n = 3$–4). *$P < 0.05$ compared with no addition.

by means of the second-derivative maximum method, using LightCycler analysis software version 3.5 and β-actin as invariant control. The primer sequences used are listed in Supplementary Table 1 (at http://www.BiochemJ.org/bj/404/bj4040499add.htm).

Statistics

The results are expressed as means ± S.E.M. for the indicated number of separate experiments. The statistical significance of differences was calculated using the Student's *t* test or ANOVA followed by Fisher's protected least significant post-hoc test (Statview 5.0.1.; SAS Institute).

RESULTS

Inhibition of JO_2 by AICA riboside in rat hepatocytes

In a first set of experiments we studied the time-course of AICA riboside effects on intracellular ZMP accumulation, AMPK activation and cellular JO_2. As expected [2,4], incubation of hepatocytes with 1 mM AICA riboside resulted in a progressive increase in intracellular ZMP level (up to 20–25 μmol · g of dry cells^{-1} after 30 min) with a parallel decrease in the concentration of AICA riboside in the medium, presumably due to its phosphorylation by adenosine kinase (Figures 1A and 1B). The activation of AMPK was very rapid and maximal within 2.5 min of incubation (Figure 1C), suggesting that modest (<3 μmol · g of dry cells^{-1}) intracellular accumulation of ZMP would be sufficient to activate AMPK. This was confirmed by the concomitant increase in the phosphorylation state of ACC, one of the main downstream targets of AMPK (Figure 1C, inset). Interestingly, in parallel with ZMP accumulation, AICA riboside decreased JO_2 of intact hepatocytes, this effect being slower than AMPK activation and maximal after about 20 min (Figure 1D).

Incubation of hepatocytes with increasing concentrations of AICA riboside was then performed in order to investigate the mechanism of inhibition of JO_2 by the nucleoside. After 30 min of incubation, AICA riboside induced a dose-dependent inhibition of the basal JO_2 (Table 1), which was already detectable at 0.05 mM AICA riboside. This effect was abolished after addition of oligomycin, an inhibitor of the F0 subunit of ATP synthase, suggesting that the inhibition of JO_2 by AICA riboside was probably due to an alteration of a mitochondrial process linked to ATP synthesis. In agreement with this interpretation, we observed that the calculated oligomycin-sensitive JO_2 (basal JO_2 minus oligomycin-insensitive JO_2), which represents the cellular oxygen consumption linked to ATP synthesis, was indeed significantly decreased whatever the concentration of AICA riboside used (Table 1). Furthermore, addition of DNP, which uncouples the mitochondrial OXPHOS, increased JO_2, even in the presence of AICA riboside. This clearly indicates that the inhibitory effect of AICA riboside on JO_2 was not present when the thermodynamic constraint on ATP synthesis was abolished by uncoupling, except at high concentrations of the nucleoside. Finally, the lack of effect of AICA riboside in the presence of TMPD/ascorbate, which assesses the maximal activity of COX, indicated

Table 1 Dose-dependent effects of AICA riboside on AMPK activity, ZMP concentration and JO_2 in isolated rat hepatocytes

Hepatocytes isolated from 24 h-starved rats were incubated at 37 °C in a Krebs/bicarbonate medium supplemented with 20 mM lactate, 2 mM pyruvate and 4 mM octanoate and in the presence or absence of the indicated concentrations of AICA riboside. After 30 min of incubation, the antimycin-sensitive JO_2 was measured before and after the successive addition of 6 μg/ml oligomycin, 100 μM DNP, 0.15 μg/ml antimycin and 1 mM TMPD plus 5 mM ascorbate. The oligomycin-sensitive JO_2 was calculated by subtracting the oligomycin-insensitive JO_2 from the basal JO_2. In separate experiments, samples of cell suspension were removed for the AMPK assay and determination of intracellular ZMP concentrations, as described in the Materials and methods section. The results are expressed as means ± S.E.M. ($n = 4$). *$P < 0.05$ compared with no addition.

AICA riboside (μM)	ZMP (μmol · g of dry hepatocytes^{-1})	AMPK activity (μmol · g of dry hepatocytes^{-1})	JO_2 (μmol O_2 · min^{-1} · g of dry hepatocytes^{-1})				
			Basal	Oligomycin	Oligomycin-sensitive	DNP	TMPD/a
0	< 0.1	123 ± 6	26.4 ± 1.3	9.9 ± 0.8	16.5 ± 1.0	44.3 ± 3.8	108.2 ± 7.1
50	1.2 ± 0.1*	145 ± 7*	22.4 ± 1.7*	10.0 ± 0.3	12.3 ± 1.4*	40.7 ± 1.3	108.0 ± 2.0
100	2.1 ± 0.1*	175 ± 7*	23.1 ± 1.2*	9.0 ± 0.8	14.1 ± 0.9*	41.2 ± 4.8	105.9 ± 6.2
250	6.1 ± 0.7*	217 ± 8*	20.9 ± 0.9*	9.9 ± 1.2	11.0 ± 0.5*	42.0 ± 5.9	99.6 ± 8.7
500	10.5 ± 1.3*	245 ± 8*	18.5 ± 0.9*	8.8 ± 0.7	9.7 ± 0.8*	38.8 ± 5.3	99.9 ± 8.8
1000	15.0 ± 1.4*	220 ± 12*	18.1 ± 0.4*	8.5 ± 1.1	9.6 ± 1.0*	38.6 ± 5.7	101.9 ± 6.7
2500	17.0 ± 1.0*	211 ± 9*	16.5 ± 1.0*	7.5 ± 0.9*	9.0 ± 0.6*	35.2 ± 5.7*	97.7 ± 6.0

Table 2 Dose-dependent effects of AICA riboside on adenine nucleotide and inorganic phosphate concentrations in isolated rat hepatocytes

Hepatocytes isolated from 24 h-starved rats were incubated as described in Table 1. After 30 min of incubation, samples of cell suspension were removed for determination of intracellular adenine nucleotide and P_i concentrations, as described in the Materials and methods section. The results are expressed as means ± S.E.M. ($n = 3$–4). *$P < 0.05$ compared with no addition; nd, not determined.

AICA riboside (μM)	(μmol · g of dry hepatocytes^{-1})					
	ATP	ADP	AMP	ΣAN	P_i	ATP/ADP
0	9.5 ± 0.3	0.7 ± 0.0	2.9 ± 0.5	13.2 ± 0.8	11.8 ± 0.6	14.4 ± 0.9
50	8.7 ± 0.5	0.8 ± 0.1	2.3 ± 0.3	11.7 ± 0.7	nd	13.2 ± 2.0
100	8.8 ± 0.6	0.7 ± 0.1	2.6 ± 0.5	12.2 ± 1.1	11.5 ± 0.9	13.4 ± 1.7
250	8.1 ± 0.6*	0.8 ± 0.1*	2.0 ± 0.2*	11.3 ± 0.7*	nd	10.4 ± 1.0*
500	8.0 ± 0.6*	0.9 ± 0.1*	1.6 ± 0.3*	10.4 ± 0.9*	4.2 ± 0.5*	9.5 ± 1.1*
1000	7.4 ± 0.7*	1.2 ± 0.2*	1.7 ± 0.3*	9.9 ± 1.0*	3.7 ± 0.6*	8.0 ± 1.3*
2500	7.2 ± 0.8*	1.1 ± 0.2*	1.6 ± 0.3*	9.9 ± 1.3*	3.4 ± 0.2*	7.4 ± 1.4*

that the nucleoside did not affect this complex of the mitochondrial respiratory chain (Table 1). Taken together, our results suggest that the inhibition of cellular JO_2 by AICA riboside was exerted on step(s) linked to ATP synthesis rather than on the electron transfer chain.

Because AICA riboside could interfere with ATP synthesis, the concentration of adenine nucleotides were measured. The dose-dependent inhibition of JO_2 by AICA riboside was accompanied by a decrease in ATP and AMP, a slight increase in ADP, and a decrease in the total concentration of adenine nucleotides (Table 2). The ATP-to-ADP ratio was significantly decreased by AICA riboside at concentrations greater than 0.1 mM. Furthermore, at these concentrations of AICA riboside, there was also a large decrease in intracellular P_i. Under these conditions, the gluconeogenic and ketogenic fluxes were drastically reduced, thus reflecting the perturbations in cellular energy metabolism induced by AICA riboside (results not shown).

Interestingly, the inhibition of oligomycin-sensitive JO_2 by AICA riboside was observed whatever the substrates used and was also reversed by DNP addition, except in the presence of glucose alone (Table 3).

Table 3 Effects of AICA riboside on oligomycin-sensitive and uncoupled JO_2 in isolated rat hepatocytes incubated with different substrates

Hepatocytes isolated from 24 h-starved rats were incubated at 37 °C in a Krebs/bicarbonate medium in the presence or absence of 1 mM AICA riboside. Experiments were performed either without the addition of exogenous substrate or in the presence of 20 mM glycerol, 20 mM glucose, 20 mM lactate, 2 mM pyruvate and 4 mM octanoate as indicated. After 30 min, the oligomycin-sensitive and uncoupled JO_2 was determined after addition of 6 μg/ml oligomycin and 100 μM DNP respectively. The results are expressed as means ± S.E.M. ($n = 4$). *$P < 0.05$ compared with no addition.

	AICA riboside	JO_2 (μmol · min^{-1} · g of dry hepatocytes^{-1})	
		Oligomycin-sensitive	DNP
Endogenous	–	3.1 ± 0.3	16.7 ± 1.0
	+	2.4 ± 0.4*	17.0 ± 0.7
Glycerol	–	5.4 ± 0.5	19.9 ± 0.7
	+	4.3 ± 0.4*	21.8 ± 1.0
Glucose	–	6.8 ± 0.8	26.1 ± 0.5
	+	2.9 ± 0.2*	19.3 ± 1.5*
Glucose + octanoate	–	12.8 ± 1.2	32.6 ± 3.5
	+	7.9 ± 0.5*	28.0 ± 0.8
Lactate + pyruvate + octanoate	–	15.2 ± 1.0	43.5 ± 3.7
	+	6.3 ± 0.7*	40.7 ± 7.1

The inhibition of JO_2 by AICA riboside is independent of AMPK

To evaluate AMPK involvement in the inhibitory effect of AICA riboside on JO_2, we resorted to engineered mice that were totally deficient in the α_1 isoform of the AMPK catalytic subunit and whose expression of the α_2 isoform was specifically deleted in the liver by Cre-recombinase technology (AMPK$\alpha_1\alpha_{2LS}^{-/-}$). We first confirmed that incubation of hepatocytes isolated from wild-type mice with 1 mM AICA riboside led to AMPK activation (Figure 2A) and decreased both oligomycin-sensitive JO_2 (Figure 2C) and ATP (Figure 2B). The extent of these effects was similar to those observed in rat hepatocytes and the inhibition

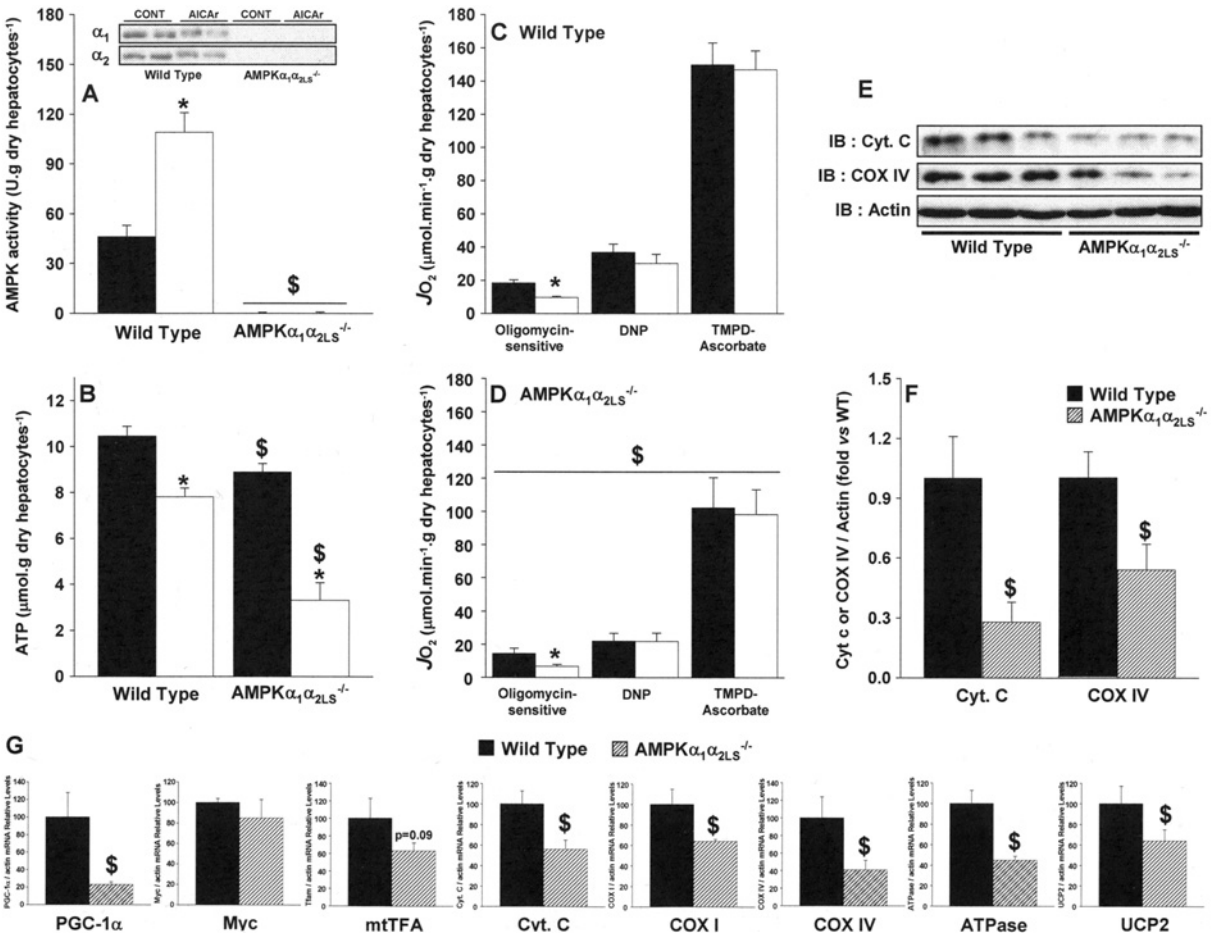

Figure 2 Effects of AICA riboside on AMPK activity, intracellular ATP concentration, oligomycin-sensitive JO_2 in hepatocytes from wild-type and AMPK$\alpha_1\alpha_{2LS}^{-/-}$ mice, and determination of hepatic expression of various mitochondrial proteins in both strains.

Hepatocytes from wild-type or AMPK$\alpha_1\alpha_{2LS}^{-/-}$ mice were incubated with 1 mM AICA riboside (□) or the vehicle (■), as described in Table 1. After 30 min, cell samples were removed for measurement of AMPK activity (**A**) and intracellular ATP concentrations (**B**). The oligomycin-sensitive JO_2 was measured in separate experiments in wild-type (**C**) and AMPK$\alpha_1\alpha_{2LS}^{-/-}$ mice (**D**), after the successive addition of 6 μg/ml oligomycin, 100 μM DNP, 0.15 μg/ml antimycin and 1 mM TMPD plus 5 mM ascorbate. The antimycin-sensitive JO_2 was calculated by subtracting the antimycin-insensitive JO_2. The cytochrome c (Cyt. C) and COX IV content in hepatocytes from wild-type (solid bars) and AMPK$\alpha_1\alpha_{2LS}^{-/-}$ (hatched bars) mice were evaluated by Western blot and quantification was performed by densitometry using actin as a loading control (**E** and **F**). RNA was extracted from freeze-clamped livers of wild-type (solid bars) and AMPK$\alpha_1\alpha_{2LS}^{-/-}$ (hatched bars) mice starved for 24 h. Quantitative real-time PCR was performed on cDNA and the mRNA contents for the indicated gene (**G**) were normalized for β-actin and expressed relative to that in wild-type mice. The results of all experiments are expressed as means ± S.E.M. ($n = 3$–5). *$P < 0.05$ compared with no addition. \$$P < 0.05$ compared with wild-type mice.

of JO_2 by AICA riboside was also reversed by addition of DNP (Figure 2C). In hepatocytes from AMPK$\alpha_1\alpha_{2LS}^{-/-}$ mice, AMPK expression, activity and activation could not be detected (Figure 2A) but the inhibition of the oligomycin-sensitive JO_2 by AICA riboside persisted (Figure 2D), excluding an effect mediated by AMPK.

Interestingly, the significant decrease in basal JO_2 evident in AMPK$\alpha_1\alpha_{2LS}^{-/-}$ mice compared with wild-type mice (Figures 2C and 2D) seemed to be due to a lower total oxidative capacity linked to a decreased cellular mitochondrial content. Indeed, we found a significant decrease in protein expression of both cytochrome *c* and COX subunit IV in AMPK$\alpha_1\alpha_{2LS}^{-/-}$ mice compared with wild-type mice (Figure 2E–2F). Note that, the basal level of ATP in AMPK$\alpha_1\alpha_{2LS}^{-/-}$ mice was also significantly lower than in wild-type mice and the decrease induced by AICA riboside was even more pronounced. These results are in agreement with those previously reported for primary cultures of hepatocytes from wild-type and AMPK$\alpha_1\alpha_{2LS}^{-/-}$ mice treated with AICA riboside [15]. The decrease in hepatic mitochondrial content evident in AMPK$\alpha_1\alpha_{2LS}^{-/-}$ mice, which is also confirmed by a significant decrease in citrate synthase activity (114 ± 6 compared with 85 ± 5 μmol · min^{-1} · g of protein^{-1} in wild-type and AMPK$\alpha_1\alpha_{2LS}^{-/-}$ mice respectively; $P < 0.05$), could be due to an alteration of mitochondrial biogenesis since liver expression of most of the genes involved in this pathway were reduced (Figure 2G), including the key transcriptional cofactor PGC-1α (peroxisome activated receptor γ coactivator-1α).

Lack of inhibition of mitochondrial oxidative phosphorylation by AICA riboside in permeabilized hepatocytes

The effect of AICA riboside in intact cells from wild-type and AMPK$\alpha_1\alpha_{2LS}^{-/-}$ mice was further investigated after permeabilization of the plasma membrane by digitonin, allowing the mitochondrial OXPHOS pathway to be investigated *in situ*. Mean values of mitochondrial antimycin-sensitive respiratory rates are given in Table 4. In the presence of glutamate/malate, a substrate for the respiratory chain complex I, no significant difference in mitochondrial respiratory rates could be detected after AICA riboside pre-treatment in both wild-type and AMPK$\alpha_1\alpha_{2LS}^{-/-}$ mice,

Table 4 Effects of AICA riboside on mitochondrial OXPHOS in permeabilized hepatocytes from wild-type and AMPK$\alpha_1\alpha_{2LS}^{-/-}$ mice

Hepatocytes from wild-type and AMPK$\alpha_1\alpha_{2LS}^{-/-}$ mice were incubated at 37 °C in the presence or absence of 1 mM AICA riboside, as described in Table 1, and then permeabilized in a KCl medium containing 200 μg/ml digitonin. After 3 min, cells were transferred to an oxygraph vessel and '*in situ*' mitochondria were energized with either 5 mM glutamate + 2.5 mM malate or 5 mM succinate + 0.5 mM malate + 1.25 μM rotenone. The state 3 respiratory rate was obtained by the addition of 1 mM ADP; the state 4 respiratory rate was obtained by the addition of 6 μg/ml oligomycin; and the uncoupled respiratory rate was obtained by the addition of 75 μM DNP. The maximal activity of COX was obtained by the addition of 1 mM TMPD and 5 mM ascorbate in the presence of 0.15 μg/ml antimycin. The antimycin-sensitive respiratory rate was calculated by subtracting the antimycin-insensitive respiratory rate. The results are expressed as means ± S.E.M. ($n = 4$–5 in each group). $^{\$}P < 0.05$ compared with wild-type. nd, not determined.

		Respiratory rate (natoms O · min^{-1} · mg of proteins^{-1})			
	AICA riboside	State 3	State 4	DNP	TMPD/a
Glutamate/malate					
Wild-type	−	62.6 ± 9.0	7.7 ± 1.4	50.5 ± 8.1	147.3 ± 23.0
	+	52.3 ± 8.6	6.3 ± 0.5	44.1 ± 9.5	140.5 ± 18.5
AMPK$\alpha_1\alpha_{2LS}^{-/-}$	−	27.7 ± 8.9$^{\$}$	3.1 ± 0.5$^{\$}$	25.1 ± 8.4$^{\$}$	89 ± 17.3$^{\$}$
	+	16.2 ± 8.4$^{\$}$	2.1 ± 0.5$^{\$}$	14.7 ± 7.9$^{\$}$	67.5 ± 19.4$^{\$}$
Succinate/malate					
Wild-type	−	68.5 ± 9.9	20.7 ± 2.3	55.4 ± 9.0	nd
	+	71.6 ± 12.6	22.5 ± 3.2	58.1 ± 11.7	nd
AMPK$\alpha_1\alpha_{2LS}^{-/-}$	−	29.3 ± 8.9$^{\$}$	10.5 ± 2.6$^{\$}$	27.2 ± 8.4$^{\$}$	nd
	+	22.0 ± 8.4$^{\$}$	8.4 ± 2.6$^{\$}$	19.4 ± 8.4$^{\$}$	nd

whatever the mitochondrial energy state. Similar results were obtained with succinate/malate, a substrate for the respiratory chain complex II. Taken together, these results demonstrate that the inhibition of JO_2 by AICA riboside required cell integrity and was lost in permeabilized cells. The results were similar in AMPK$\alpha_1\alpha_{2LS}^{-/-}$ and also confirmed an overall decrease in mitochondrial respiration in hepatocytes compared with wild-type mice.

Mechanism of inhibition of OXPHOS by AICA riboside in intact cells

The lack of inhibition of respiration by AICA riboside in permeabilized hepatocytes suggested that the inhibition in intact cells could result from the intracellular accumulation of low-molecular-mass compounds, such as Z nucleotides, that could have been lost by permeabilization. We first investigated the effects of Z nucleotides on the mitochondrial OXPHOS pathway (Table 5). In rat mitochondria energized with glutamate/malate, but not with succinate/malate, ZMP significantly inhibited state 3 respiration. This inhibition persisted in the presence of DNP, which was not the case in intact cells. In addition, incubation of disrupted mitochondria with ZMP significantly decreased the specific activity of the respiratory chain complex I (78 ± 4, 69 ± 4 and 62 ± 3 nmol · min^{-1} · mg of protein^{-1} for control, 1 mM ZMP and 2.5 mM ZMP respectively; $P < 0.05$), demonstrating a direct inhibition of this mitochondrial complex by the nucleotide. In contrast, ZTP stimulated mitochondrial respiration whatever the substrate and the mitochondrial energy states (Table 5). Alternatively, the inhibition of oligomycin-sensitive JO_2 could result from the AICA riboside-induced depletion of substrates for the mitochondrial OXPHOS, such as adenine nucleotides and P_i. This situation is reminiscent of the depletion of adenine nucleotides induced by fructose in hepatocytes [25]. To test this hypothesis, we evaluated the effect of AICA riboside on JO_2 in hepatocytes pre-incubated with 5 mM fructose to decrease intracellular P_i (Table 6). Fructose pre-treatment indeed worsened the relative inhibition of oligomycin-sensitive JO_2 by AICA riboside (−51 % compared with −63 %; $P < 0.05$, control compared with fructose). In these cells, pre-incubation with fructose also worsened the AICA riboside-induced depletion of ATP and total adenine nucleotides and decreased the ATP-to-ADP ratio, thus making it difficult to unequivocally assign to P_i depletion of the inhibition of cellular respiration.

Table 5 Effects of AICA riboside and Z nucleotides on OXPHOS in rat isolated mitochondria

Isolated rat mitochondria (1 mg/ml) were incubated at 37 °C in a KCl medium in the presence of 1 mM AICA riboside, the indicated concentrations of nucleotides or the vehicle. Mitochondria were energized with either 5 mM glutamate + 2.5 mM malate or 5 mM succinate + 0.5 mM malate + l.25 μM rotenone. The state 3 respiratory rate was obtained by the addition of 1 mM ADP; the state 4 respiratory rate was obtained by the addition of 6 μg/ml oligomycin; and the uncoupled respiratory rate was obtained by the addition of 75 μM DNP. Antimycin-sensitive JO_2 was calculated by subtracting the antimycin-insensitive respiratory rate after addition of 0.15 μg/ml antimycin. The results are expressed as means ± S.E.M. ($n = 3$–4 different preparations, each assay being performed in duplicate). $^{*}P < 0.05$ compared with control (vehicle).

	Respiratory rate (natoms O · min^{-1} · mg of proteins^{-1})		
	State 3	State 4	DNP
Glutamate/malate			
Control	80.7 ± 3.0	15.9 ± 0.6	126.0 ± 5.9
AICA riboside	80.5 ± 8.2	16.4 ± 0.9	120.0 ± 14.2
1 mM ZMP	74.0 ± 1.3*	15.4 ± 0.3	105.3 ± 1.2*
2.5 mM ZMP	61.5 ± 5.0*	15.7 ± 1.5	98.6 ± 4.2*
0.5 mM ZTP	97.1 ± 8.7*	19.7 ± 0.8*	138.5 ± 9.2*
1 mM ZTP	105.1 ± 8.4*	23.7 ± 1.6*	144.3 ± 13.0*
Succinate/malate			
Control	122.9 ± 0.6	37.6 ± 0.2	158.0 ± 7.1
AICA riboside	120.0 ± 3.0	35.6 ± 0.9	143.1 ± 4.9
1 mM ZMP	122.3 ± 4.7	34.8 ± 0.7	140.7 ± 1.2
0.5 mM ZTP	122.1 ± 5.5	41.9 ± 2.1*	210.2 ± 9.5*

To assess the importance of adenine nucleotide depletion in the AICA riboside-induced inhibition of JO_2, we resorted to coformycin, a known inhibitor of AMP deaminase. This enzyme is inhibited by P_i and limits the breakdown of adenine nucleotides in the liver. Therefore any depletion of intracellular P_i relieves the inhibition of AMP deaminase and favours adenine nucleotide breakdown, as it occurs in fructose or AICA riboside treated hepatocytes (Table 6). Pre-incubation of hepatocytes with 10 μM coformycin prevented ATP and total adenine nucleotide depletion, but did not affect the AICA riboside-induced P_i drop (−65 % compared with −62 %), the decrease in the ATP-to-ADP ratio and the inhibition of oligomycin-sensitive JO_2 (Table 6).

Table 6 Effects of fructose and coformycin on the AICA riboside-induced decrease in oligomycin-sensitive JO_2 and adenine nucleotide, ZMP and P_i concentrations in rat hepatocytes

Hepatocytes isolated from 24 h-starved rats were incubated at 37 °C in a Krebs/bicarbonate medium supplemented with 20 mM lactate, 2 mM pyruvate and 4 mM octanoate in the presence or absence of 5 mM fructose or 10 μM coformycin. After 15 min of preincubation, AICA riboside (1 mM final concentration) or its vehicle were added and cell samples were removed 30 min later for determination of the oligomycin-sensitive JO_2, as described in the legend of Figure 2. Determination of adenine nucleotides, ZMP and P_i were performed in separate experiments. The results are expressed as means ± S.E.M. ($n = 3$). *$P < 0.05$ compared with no AICA riboside addition; $^{\$}P < 0.05$ compared with control incubated in the same conditions.

	AICA riboside	ZMP (μmol · g of dry hepatocytes^{-1})	JO_2 (μmol · min^{-1} · g of dry hepatocytes^{-1})	(μmol · g dry hepatocytes^{-1}) ATP	ADP	AMP	ΣAN	P_i	ATP/ADP
Control	−	< 0.1	17.8 ± 0.4	10.4 ± 0.4	0.9 ± 0.1	3.5 ± 0.3	15.1 ± 0.5	12.6 ± 0.1	13.2 ± 1.6
	+	21.2 ± 1.1*	8.7 ± 0.6*	8.4 ± 0.5*	1.7 ± 0.1*	2.5 ± 0.2*	12.2 ± 0.7*	4.4 ± 0.1*	5.1 ± 0.4*
Fructose	−	< 0.1	20.0 ± 1.1$^{\$}$	7.4 ± 0.4$^{\$}$	1.0 ± 0.1	2.8 ± 0.2$^{\$}$	11.3 ± 0.6$^{\$}$	17.4 ± 0.8$^{\$}$	8.7 ± 1.3$^{\$}$
	+	6.1 ± 0.1*$^{\$}$	7.4 ± 0.6*$^{\$}$	3.3 ± 0.2*$^{\$}$	1.7 ± 0.2*	2.9 ± 0.2	7.7 ± 0.5*$^{\$}$	2.4 ± 0.3*$^{\$}$	2.1 ± 0.2*$^{\$}$
Coformycin	−	< 0.1	15.0 ± 0.3$^{\$}$	12.3 ± 0.2$^{\$}$	1.2 ± 0.1$^{\$}$	4.3 ± 0.2$^{\$}$	18.2 ± 0.3$^{\$}$	11.3 ± 0.3$^{\$}$	12.1 ± 1.0
	+	13.2 ± 0.3*$^{\$}$	8.5 ± 0.8*	12.9 ± 0.2$^{\$}$	3.0 ± 0.1*$^{\$}$	3.7 ± 0.4$^{\$}$	19.5 ± 0.5$^{\$}$	4.3 ± 0.3*	4.7 ± 0.2*

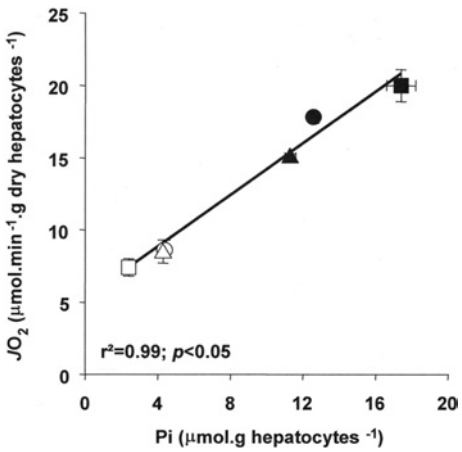

Figure 3 Relationship between intracellular Pi and oligomycin-sensitive respiration in hepatocytes

Hepatocytes were incubated as described in Table 6 with (open symbols) or without (closed symbols) 1 mM AICA riboside and in the presence of fructose (■,□), coformycin (▲,△) or vehicle (●,○). The results are expressed as means ± S.E.M. ($n = 3$).

Taken together these results suggest that the depletion of P_i that follows phosphorylation of AICA riboside into ZMP also participates in the inhibition of cellular respiration by the nucleoside. Finally, the clear relationship evident between intracellular P_i and oligomycin-sensitive JO_2 (Figure 3) further reinforces this proposed mechanism.

DISCUSSION

We report in the present study that AICA riboside, which is classically used to activate AMPK in cells, was unexpectedly found to inhibit respiration in intact hepatocytes. This effect was readily observed at concentrations of AICA riboside greater than 0.1 mM and was clearly not mediated by AMPK since it persisted in hepatocytes isolated from AMPK$\alpha_1\alpha_{2LS}^{-/-}$ mice. We propose that this inhibition resulted from the combined decrease in intracellular P_i concentration and the accumulation of Z nucleotides following AICA riboside phosphorylation. Incubation of hepatocytes with AICA riboside induced major changes in nucleotides and P_i content similar to those caused by the accumulation of Fru-1-P (fructose 1-phosphate) and Gly-3-P (glycerol 3-phosphate) in hepatocytes incubated with fructose [25] and glycerol [26] respectively. ZMP resulting from the phosphorylation of AICA riboside by adenosine kinase acts as a P_i trap, in a similar manner to Fru-1-P and Gly-3-P, thus leading to depletion of free P_i and adenine nucleotides. Indeed, an approximate estimation of the intracellular phosphate charge indicates that the amount of free and adenine nucleotide-bound P_i decreased from about 45 μmol · g of dry cells^{-1} in controls to about 30 μmol · g of dry cells^{-1} after incubation with 1 mM AICA riboside, the difference being recovered in the Z nucleotides, mainly ZMP (Tables 1 and 2). This is in agreement with a previous report [27] showing that the liver concentration of free P_i decreased by 50 % after *in vivo* administration of AICA riboside and was accompanied by a concomitant and dose-dependent drop in ATP levels owing to the marked accumulation of phosphorylated compounds. The immediate consequence of this P_i depletion is the de-inhibition of AMP deaminase, resulting in the loss of adenine nucleotides (Table 2), and the expected breakdown of the purine ring into allantoin, as previously reported [28,29]. Interestingly, use of coformycin, an inhibitor of AMP deaminase, abolishes the AICA riboside-induced decrease in adenine nucleotides, but not of P_i and JO_2 (Table 6).

Collectively, the results of the present study suggest that the main changes induced by AICA riboside, namely the accumulation of ZMP and the depletion of intracellular P_i, are responsible for the inhibition of cellular respiration. In intact cells incubated with lactate/pyruvate and octanoate as substrates, the decrease in JO_2 induced by AICA riboside was relieved under uncoupled conditions, i.e. the addition of DNP, indicating that the inhibition was mainly exerted on respiration coupled to ATP synthesis in this condition. Since JO_2 is expected to slow down when the concentration of mitochondrial OXPHOS cofactors are limiting [30], the massive drop in P_i following AICA riboside phosphorylation constitutes an attractive explanation. The tight relationship observed between its intracellular content and the oligomycin-sensitive JO_2 illustrates this functional hypothesis.

Accumulation of Z nucleotides, which occurred in all AICA riboside-treated cells, could also participate in the inhibition through a direct effect on the mitochondrial respiratory chain. ZMP was indeed found to inhibit complex I of the respiratory chain in isolated liver mitochondria (Table 4). Such an effect would decrease JO_2 in intact hepatocytes, even after addition of the uncoupler DNP, since inhibition of complex I induces kinetic constraint on the entire electron transport chain. However, inhibition of JO_2 by AICA riboside in the presence of DNP was only

observed with glucose alone, a substrate almost exclusively providing NADH to the mitochondrial respiratory chain complex I. In hepatocytes incubated with substrates providing both NADH and $FADH_2$ with a closely related stochiometry, i.e. glycerol or fatty acid, this effect was probably masked, except at very high concentrations, because of the partial bypass of complex I [31]. In addition, ZTP, which accumulates in hepatocytes theoretically 10-fold less than ZMP [2], induced stimulation of mitochondrial state 4 respiratory rate. This suggests an uncoupling of mitochondrial OXPHOS (Table 4), an effect that could also worsen the change in cellular energetics by decreasing the yield of ATP synthesis. Importantly, all of these effects were observed at concentrations of ZMP and ZTP in the range of those detected in isolated hepatocytes incubated with AICA riboside. Indeed, assuming an intracellular water content of $2\ ml \cdot g^{-1}$ of dry weight, in cells exposed for 30 min to 1 mM AICA riboside, ZMP and ZTP can reach intracellular concentrations higher than 7.5 and 0.75 mM respectively. Finally, although OXPHOS inhibition by AICA riboside can readily be explained by the observed changes in P_i and ZMP concentrations, other effects of Z nucleotides, e.g. on ATP synthase, adenine nucleotide translocator or P_i transporter, are not excluded.

It is important to note that the inhibition of oligomycin-sensitive respiration by AICA riboside was not restricted to hepatocytes and was also observed in various cell lines, including C2C12, CaCo-2, KB and also human endothelial cells (e.g. HMEC-1; results not shown). The common phenomenon shared by these cells is their capacity to accumulate ZMP, but the extent of JO_2 inhibition induced by AICA riboside was rather low compared with fresh hepatocytes. However, these culture cell lines generally exhibit high glycolytic rates and are therefore less dependent on mitochondrial OXPHOS for ATP supply. The energetic consequences of the AMPK-independent inhibition of OXPHOS by AICA riboside in these cells are therefore expected to be less important than in liver cells. Thus the alteration of the OXPHOS pathway by AICA riboside and the subsequent intracellular ATP drop could be explained, at least in part, by the detrimental effect of the nucleoside treatment evident in highly aerobic tissues, i.e. in the liver [32] or pancreatic cells [33,34]. In contrast, we suggest that the protection against apoptosis exerted by AICA riboside in some culture cell lines [35–37] could be due to subtle mitochondrial modifications induced by Z nucleotides. Indeed, moderate inhibition of electron flux through the respiratory chain complex I, as observed with ZMP, has been demonstrated to protect cells against oxidative stress-induced cell death [21,38].

It is obvious from our results that caution should be exerted when interpreting the results obtained with AICA riboside and assumed to result from AMPK activation. Among the AMPK-independent but AICA riboside-induced effect, intracellular accumulation of ZMP has also been reported to directly modulate enzymes with AMP-binding sites, such as glucokinase [39], glycogen phosphorylase [40,41], glycogen synthase [40] or fructosew 1,6-bisphosphatase [2]. The K_m values of these enzymes for ZMP were indeed generally in the range of the cellular nucleotide concentration, a point which was often overlooked in the interpretation of the results obtained with AICA riboside. Two recent papers have also reported AMPK-independent effects of AICA riboside on hepatic phosphatidylcholine synthesis [42] and autophagic proteolysis [43], without however providing any mechanistic explanation for these non-specific effects.

The striking lower basal JO_2 in hepatocytes from $AMPK\alpha_1\alpha_{2LS}^{-/-}$ compared with wild-type mice is probably due to a decrease in mitochondrial content rather than a qualitative modification of the mitochondrial machinery. Indeed, no differences were evident in both cellular (Figure 2) and mitochondrial (Table 4) respiration when the results were normalized using the maximal activity of COX (results not shown), a usual marker of cellular mitochondrial density. AMPK has been reported to be involved in muscle mitochondrial biogenesis [13,14] and our results suggest, for the first time, that this is also the case for the liver. Indeed, the deletion of both AMPKα subunits in hepatocytes leads to reduced mitochondrial respiration and decreased transcript and protein expression of key mitochondrial constituents, delineating an apparent alteration of the starvation-induced activation of the mitochondrial biogenesis programme in the liver of these mice. PGC-1α [44] and myc [45] have recently been identified as key transcriptional cofactors involved in this pathway since they co-ordinate activation of several transcription factors, including nuclear respiratory factors and mtTFA (mitochondrial transcription factor A), which in turn enhances expression of nuclear and mitochondrial genes encoding mitochondrial proteins [46]. While the mRNA content of myc was not modified, the expression of PGC-1α, together with numbers of nuclear [COX IV, cytochrome *c*, UCP2 (uncoupling protein 2), ATPase] and mitochondrial (COX I) genes, was drastically reduced in $AMPK\alpha_1\alpha_{2LS}^{-/-}$ mice (Figure 2). The mechanisms by which deletion of AMPK in the liver affects PGC-1α expression and mitochondrial biogenesis remain to be elucidated.

In conclusion, while one might consider short-term incubations with low concentrations (< 0.1 mM) of AICA riboside to activate AMPK with little OXPHOS damage, we believe that this compound is not well-suited to investigate the consequences of AMPK activation on various cell functions because of its misleading side-effects. Other more specific tools and/or new pharmacological compounds with better AMPK selectivity are required. Among these, genetic approaches including overexpression of negative or constitutively active forms of AMPK [47], use of small interfering RNA [48], and invalidation of the genes coding for the catalytic subunits of the kinase [49] are to be considered, taking into account their inherent limitations. Alternatively, the recent development of new activators of AMPK, apparently devoid of any apparent effect on adenine nucleotide content in primary cultured hepatocytes [50], is of direct interest.

This work was supported by FNRS, the French Community of Belgium, the Belgian Federal Program Interuniversity Poles of Attraction (P5) and the European Union FP6 programme (Exgenesis, LSHM-CT-2004-005272). B. G. is a recipient of the ICP-'Michel de Visscher' Fellowship and N.T. is recipient of a French EURODOC grant of the Région Rhône-Alpes. The authors are grateful to Liliane Maisin and Martine de Cloedt for technical assistance.

REFERENCES

1 Zimmerman, T. P. and Deeprose, R. D. (1978) Metabolism of 5-amino-1-β-D-ribofuranosylimidazole-4-carboxamide and related five-membered heterocycles to 5′-triphosphates in human blood and L5178Y cells. Biochem. Pharmacol. **27**, 709–716
2 Vincent, M. F., Marangos, P. J., Gruber, H. E. and Van den Berghe, G. (1991) Inhibition by AICA riboside of gluconeogenesis in isolated rat hepatocytes. Diabetes **40**, 1259–1266
3 Sullivan, J. E., Brocklehurst, K. J., Marley, A. E., Carey, F., Carling, D. and Beri, R. K. (1994) Inhibition of lipolysis and lipogenesis in isolated rat adipocytes with AICAR, a cell-permeable activator of AMP-activated protein kinase. FEBS Lett. **353**, 33–36
4 Corton, J. M., Gillespie, J. G., Hawley, S. A. and Hardie, D. G. (1995) 5-Aminoimidazole-4-carboxamide ribonucleoside: a specific method for activating AMP-activated protein-kinase in intact cells. Eur. J. Biochem. **229**, 558–565
5 Christopher, M., Rantzau, C., Chen, Z. P., Snow, R., Kemp, B. and Alford, F. P. (2006) Impact of *in vivo* fatty acid oxidation blockade on glucose turnover and muscle glucose metabolism during low-dose AICAR infusion. Am. J. Physiol. Endocrinol. Metab. **291**, E1131–E1140
6 Aschenbach, W. G., Hirshman, M. F., Fujii, N., Sakamoto, K., Howlett, K. F. and Goodyear, L. J. (2002) Effect of AICAR treatment on glycogen metabolism in skeletal muscle. Diabetes **51**, 567–573

7 Bergeron, R., Previs, S. F., Cline, G. W., Perret, P., Russell, 3rd, R.R., Young, L.H. and Shulman, G.I. (2001) Effect of 5-aminoimidazole-4-carboxamide-1-β-D-ribofuranoside infusion on *in vivo* glucose and lipid metabolism in lean and obese Zucker rats. Diabetes **50**, 1076–1082

8 Iglesias, M. A., Furler, S. M., Cooney, G. J., Kraegen, E. W. and Ye, J. M. (2004) AMP-activated protein kinase activation by AICAR increases both muscle fatty acid and glucose uptake in white muscle of insulin-resistant rats *in vivo*. Diabetes **53**, 1649–1654

9 Pencek, R. R., Shearer, J., Camacho, R. C., James, F. D., Lacy, D. B., Fueger, P. T., Donahue, E. P., Snead, W. and Wasserman, D. H. (2005) 5-Aminoimidazole-4-carboxamide-1-β-D-ribofuranoside causes acute hepatic insulin resistance *in vivo*. Diabetes **54**, 355–360

10 Hardie, D. G., Hawley, S. A. and Scott, J. W. (2006) AMP-activated protein kinase: development of the energy sensor concept. J. Physiol. **574**, 7–15

11 Viollet, B., Foretz, M., Guigas, B., Horman, S., Dentin, R., Bertrand, L., Hue, L. and Andreelli, F. (2006) Activation of AMP-activated protein kinase in the liver: a new strategy for the management of metabolic hepatic disorders. J. Physiol. **574**, 41–53

12 Reznick, R. M. and Shulman, G. I. (2006) The role of AMP-activated protein kinase in mitochondrial biogenesis. J. Physiol. **574**, 33–39

13 Bergeron, R., Ren, J. M., Cadman, K. S., Moore, I. K., Perret, P., Pypaert, M., Young, L. H., Semenkovich, C. F. and Shulman, G. I. (2001) Chronic activation of AMP kinase results in NRF-1 activation and mitochondrial biogenesis. Am. J. Physiol. Endocrinol. Metab. **281**, E1340–E1346

14 Zong, H., Ren, J. M., Young, L. H., Pypaert, M., Mu, J., Birnbaum, M. J. and Shulman, G. I. (2002) AMP kinase is required for mitochondrial biogenesis in skeletal muscle in response to chronic energy deprivation. Proc. Natl. Acad. Sci. U.S.A. **99**, 15983–15987

15 Guigas, B., Bertrand, L., Taleux, N., Foretz, M., Wiernsperger, N., Vertommen, D., Andreelli, F., Viollet, B. and Hue, L. (2006) 5-Aminoimidazole-4-carboxamide-1-β-D-ribofuranoside and metformin inhibit hepatic glucose phosphorylation by an AMP-activated protein kinase-independent effect on glucokinase translocation. Diabetes **55**, 865–874

16 Viollet, B., Andreelli, F., Jorgensen, S. B., Perrin, C., Geloen, A., Flamez, D., Mu, J., Lenzner, C., Baud, O., Bennoun, M. et al. (2003) The AMP-activated protein kinase α2 catalytic subunit controls whole-body insulin sensitivity. J. Clin. Invest. **111**, 91–98

17 Kellendonk, C., Opherk, C., Anlag, K., Schutz, G. and Tronche, F. (2000) Hepatocyte-specific expression of Cre recombinase. Genesis **26**, 151–153

18 Jorgensen, S. B., Viollet, B., Andreelli, F., Frosig, C., Birk, J. B., Schjerling, P., Vaulont, S., Richter, E. A. and Wojtaszewski, J. F. (2004) Knockout of the α2 but not α1 5′-AMP-activated protein kinase isoform abolishes 5-aminoimidazole-4-carboxamide-1-β-4-ribofuranoside but not contraction-induced glucose uptake in skeletal muscle. J. Biol. Chem. **279**, 1070–1079

19 Bontemps, F., Hue, L. and Hers, H. G. (1978) Phosphorylation of glucose in isolated rat hepatocytes. Sigmoidal kinetics explained by the activity of glucokinase alone. Biochem. J. **174**, 603–611

20 Klingenberg, M. and Slenczka, W. (1959) Pyridine nucleotide in liver mitochondria. An analysis of their redox relationships. Biochem. Z. **331**, 486–517

21 Guigas, B., Detaille, D., Chauvin, C., Batandier, C., De Oliveira, F., Fontaine, E. and Leverve, X. (2004) Metformin inhibits mitochondrial permeability transition and cell death: a pharmacological *in vitro* study. Biochem. J. **382**, 877–884

22 Srere, P. A. (1969) Methods in Enzymology, vol. 13, pp. 3–11, Academic Press, New York

23 Ichai, C., Guignot, L., El-Mir, M. Y., Nogueira, V., Guigas, B., Chauvin, C., Fontaine, E., Mithieux, G. and Leverve, X. M. (2001) Glucose 6-phosphate hydrolysis is activated by glucagon in a low temperature-sensitive manner. J. Biol. Chem. **276**, 28126–28133

24 Itaya, K. and Ui, M. (1966) A new micromethod for the colorimetric determination of inorganic phosphate. Clin. Chim. Acta **14**, 361–366

25 Van den Berghe, G., Bronfman, M., Vanneste, R. and Hers, H. G. (1977) The mechanism of adenosine triphosphate depletion in the liver after a load of fructose. A kinetic study of liver adenylate deaminase. Biochem. J. **162**, 601–609

26 Maswoswe, S. M., Daneshmand, F. and Davies, D. R. (1986) Metabolic effects of D-glyceraldehyde in isolated hepatocytes. Biochem. J. **240**, 771–776

27 Vincent, M. F., Erion, M. D., Gruber, H. E. and Van den Berghe, G. (1996) Hypoglycaemic effect of AICA riboside in mice. Diabetologia **39**, 1148–1155

28 Smith, C. M., Rovamo, L. M. and Raivio, K. O. (1977) Fructose-induced adenine nucleotide catabolism in isolated rat hepatocytes. Can. J. Biochem. **55**, 1237–1240

29 Van den Berghe, G., Bontemps, F. and Hers, H. G. (1980) Purine catabolism in isolated rat hepatocytes. Influence of coformycin. Biochem. J. **188**, 913–920

30 Brown, G. C., Lakin-Thomas, P. L. and Brand, M. D. (1990) Control of respiration and oxidative phosphorylation in isolated rat liver cells. Eur. J. Biochem. **192**, 355–362

31 Leverve, X. M. and Fontaine, E. (2001) Role of substrates in the regulation of mitochondrial function in situ. IUBMB Life **52**, 221–229

32 Meisse, D., Van de Casteele, M., Beauloye, C., Hainault, I., Kefas, B. A., Rider, M. H., Foufelle, F. and Hue, L. (2002) Sustained activation of AMP-activated protein kinase induces c-Jun N-terminal kinase activation and apoptosis in liver cells. FEBS Lett. **526**, 38–42

33 Kefas, B. A., Heimberg, H., Vaulont, S., Meisse, D., Hue, L., Pipeleers, D. and Van de Casteele, M. (2003) AICA-riboside induces apoptosis of pancreatic β cells through stimulation of AMP-activated protein kinase. Diabetologia **46**, 250–254

34 Campas, C., Lopez, J. M., Santidrian, A. F., Barragan, M., Bellosillo, B., Colomer, D. and Gil, J. (2003) Acadesine activates AMPK and induces apoptosis in B-cell chronic lymphocytic leukemia cells but not in T lymphocytes. Blood **101**, 3674–3680

35 Stefanelli, C., Stanic, I., Bonavita, F., Flamigni, F., Pignatti, C., Guarnieri, C. and Caldarera, C. M. (1998) Inhibition of glucocorticoid-induced apoptosis with 5-aminoimidazole-4-carboxamide ribonucleoside, a cell-permeable activator of AMP-activated protein kinase. Biochem. Biophys. Res. Commun. **243**, 821–826

36 Stet, E. H., De Abreu, R. A., Bokkerink, J. P., Vogels-Mentink, T. M., Lambooy, L. H., Trijbels, F. J. and Trueworthy, R. C. (1993) Reversal of 6-mercaptopurine and 6-methylmercaptopurine ribonucleoside cytotoxicity by amidoimidazole carboxamide ribonucleoside in Molt F4 human malignant T-lymphoblasts. Biochem. Pharmacol. **46**, 547–550

37 Ido, Y., Carling, D. and Ruderman, N. (2002) Hyperglycemia-induced apoptosis in human umbilical vein endothelial cells: inhibition by the AMP-activated protein kinase activation. Diabetes **51**, 159–167

38 Detaille, D., Guigas, B., Chauvin, C., Batandier, C., Fontaine, E., Wiernsperger, N. and Leverve, X. (2005) Metformin prevents high-glucose-induced endothelial cell death through a mitochondrial permeability transition-dependent process. Diabetes **54**, 2179–2187

39 Vincent, M. F., Bontemps, F. and Van den Berghe, G. (1992) Inhibition of glycolysis by 5-amino-4-imidazolecarboxamide riboside in isolated rat hepatocytes. Biochem. J. **281**, 267–272

40 Longnus, S. L., Wambolt, R. B., Parsons, H. L., Brownsey, R. W. and Allard, M. F. (2003) 5-Aminoimidazole-4-carboxamide 1-β-D-ribofuranoside (AICAR) stimulates myocardial glycogenolysis by allosteric mechanisms. Am. J. Physiol. Regul. Integr. Comp. Physiol. **284**, R936–R944

41 Shang, J. and Lehrman, M. A. (2004) Activation of glycogen phosphorylase with 5-aminoimidazole-4-carboxamide riboside (AICAR). Assessment of glycogen as a precursor of mannosyl residues in glycoconjugates. J. Biol. Chem. **279**, 12076–12080

42 Jacobs, R. L., Lingrell, S., Dyck, J. R. and Vance, D. E. (2007) Inhibition of hepatic phosphatidylcholine synthesis by 5-aminoimidazole-4-carboxamide-1-β-4-ribofuranoside (AICAR) is independent of AMP-activated protein kinase (AMPK) activation. J. Biol. Chem. **282**, 4516–4523

43 Meley, D., Bauvy, C., Houben-Weerts, J. H., Dubbelhuis, P. F., Helmond, M. T., Codogno, P. and Meijer, A. J. (2006) AMP-activated protein kinase and the regulation of autophagic proteolysis. J. Biol. Chem. **281**, 34870–34879

44 Wu, Z., Puigserver, P., Andersson, U., Zhang, C., Adelmant, G., Mootha, V., Troy, A., Cinti, S., Lowell, B., Scarpulla, R. C. and Spiegelman, B. M. (1999) Mechanisms controlling mitochondrial biogenesis and respiration through the thermogenic coactivator PGC-1. Cell **98**, 115–124

45 Li, F., Wang, Y., Zeller, K. I., Potter, J. J., Wonsey, D. R., O'Donnell, K. A., Kim, J. W., Yustein, J. T., Lee, L. A. and Dang, C. V. (2005) Myc stimulates nuclearly encoded mitochondrial genes and mitochondrial biogenesis. Mol. Cell. Biol. **25**, 6225–6234

46 Scarpulla, R. C. (2006) Nuclear control of respiratory gene expression in mammalian cells. J. Cell. Biochem. **97**, 673–683

47 Woods, A., Azzout-Marniche, D., Foretz, M., Stein, S. C., Lemarchand, P., Ferre, P., Foufelle, F. and Carling, D. (2000) Characterization of the role of AMP-activated protein kinase in the regulation of glucose-activated gene expression using constitutively active and dominant negative forms of the kinase. Mol. Cell. Biol. **20**, 6704–6711

48 Pilon, G., Dallaire, P. and Marette, A. (2004) Inhibition of inducible nitric-oxide synthase by activators of AMP-activated protein kinase: a new mechanism of action of insulin-sensitizing drugs. J. Biol. Chem. **279**, 20767–20774

49 Viollet, B., Andreelli, F., Jorgensen, S. B., Perrin, C., Flamez, D., Mu, J., Wojtaszewski, J. F., Schuit, F. C., Birnbaum, M., Richter, E., Burcelin, R. and Vaulont, S. (2003) Physiological role of AMP-activated protein kinase (AMPK): insights from knockout mouse models. Biochem. Soc. Trans. **31**, 216–219

50 Cool, B., Zinker, B., Chiou, W., Kifle, L., Cao, N., Perham, M., Dickinson, R., Adler, A., Gagne, G., Iyengar, R. et al. (2006) Identification and characterization of a small molecule AMPK activator that treats key components of type 2 diabetes and the metabolic syndrome. Cell. Metab. **3**, 403–416

Received 18 January 2007/21 February 2007; accepted 27 February 2007
Published as BJ Immediate Publication 27 February 2007, doi:10.1042/BJ20070105